

Interaction effects in the optical conductivity of bilayer graphene: Drude-interband coupling and screening

Wang-Kong Tse and A. H. MacDonald

Department of Physics, University of Texas, Austin, Texas 78712, USA

(Received 4 August 2009; revised manuscript received 19 October 2009; published 20 November 2009)

We present a theory of the influence of band renormalization and excitonic electron-electron interaction effects on the optical conductivity $\sigma(\omega)$ of doped bilayer graphene. Using the Keldysh formalism, we derive a kinetic equation from which we extract numerical and approximate analytic results for $\sigma(\omega)$. Our calculations reveal a previously unrecognized mechanism which couples the Drude and interband response and renormalizes the plasmon frequency, and suggest that screening must play an essential role in explaining the weakly renormalized conductivity seen in recent experiments.

DOI: [10.1103/PhysRevB.80.195418](https://doi.org/10.1103/PhysRevB.80.195418)

PACS number(s): 78.66.Tr, 72.20.Dp, 73.63.Bd, 78.67.Pt

I. INTRODUCTION

Experimental progress¹ over the past five years has made it possible to isolate single-layer graphene (SLG), an atomically two-dimensional electron system based on a honeycomb lattice of carbon atoms, and study its electronic properties. More recently similar techniques have been used to study multilayer graphene films and other types of graphitic nanostructures. One of the surprises in this field is that the electronic properties of Bernal stacked bilayer graphene (BLG) are quite distinct² from those of SLG. The low-energy electronic excitations of a bilayer are *massive* and have momentum-space Berry phase 2π , while those of SLG are massless and have Berry phase π .

The optical conductivity $\sigma(\omega)$ of BLG has received a lot of attention, both experimentally and theoretically. Theoretical studies³⁻⁷ of $\sigma(\omega)$ in BLG have so far entirely neglected the interactions effects that are known to be crucial in the optical response of regular semiconductors.^{8,9} The noninteracting electron interpretation of $\sigma(\omega)$ data¹⁰⁻¹³ does nevertheless appear to be generally successful, surprisingly so since BLG is generally expected to display stronger interaction effects than SLG because of its parabolic band dispersion. For example band-structure renormalizations are expected¹⁴ to be relatively modest in SLG, but substantially stronger in the BLG case. Indeed the interacting electron problem in bilayer graphene poses a number of interesting new questions because of its unique massive chiral quasiparticles.

These circumstances call for the theoretical analysis of the influence of interactions on $\sigma(\omega)$ presented in this paper. We use a quantum kinetic equation (QKE) derived using the Keldysh formalism to take electron-electron (e-e) band renormalization and excitonic effects into account on an equal footing (thus correctly guaranteeing gauge invariance). We show that although the energy dispersion of BLG is parabolic, its optical properties are very different from those of regular semiconductors or semiconductor bilayers: (i) A new coupling between the Drude (i.e., intraband) and interband optical transition channels follows from the chirality of the BLG band eigenstates; (ii) the Drude-interband coupling (DIC) is responsible for a renormalization of the leading-order long-wavelength plasmon dispersion; and (iii) because

of the chirality structure, screening is responsible for an especially strong suppression of interaction effects.

II. QUANTUM KINETIC EQUATION

States near the Fermi level of bilayer graphene are described by the two-band envelope function Hamiltonian² $H = -\epsilon_k \boldsymbol{\sigma} \cdot \mathbf{n}$, where $\epsilon_k = k^2/2m$, $\mathbf{n} = (\cos 2\phi_k, \sin 2\phi_k)$, and $\boldsymbol{\sigma}$ is the Pauli-matrix vector which acts on the layer pseudospin degrees of freedom. [We set $\hbar=1$ throughout restoring it only in the final expressions for $\sigma(\omega)$]. This Hamiltonian is valid when $v_F k \ll \gamma_1$ where $v_F \approx 10^6 \text{ ms}^{-1}$ is the quasiparticle velocity of SLG and $\gamma_1 \approx 0.4 \text{ eV}$ (Refs. 11 and 15) is the interlayer hopping amplitude. (We neglect trigonal warping, which is important only at low densities and energies.) Although conduction and valence-band eigenenergies have the same quadratic dispersion in regular semiconductors and BLG, the eigenfunction properties differ. In the BLG case the conduction and valence-band eigenstates are both linear combinations of π orbitals, whereas in the regular semiconductor case the two bands have orbitals with different atomic character. We will see that this property alone profoundly alters the $\sigma(\omega)$ theory. Furthermore bilayer graphene is gapless.¹⁶

To incorporate band renormalization and excitonic effects on an equal footing, we derive a quantum kinetic equation for bilayer graphene using the Keldysh formalism and a first-order exchange-interaction approximation for the interaction self-energy. Importantly the interaction term in the envelope function is diagonal¹⁷ in pseudospin labels at each interaction vertex. To obtain a kinetic equation, it is customary to employ a Wigner representation in which the relative coordinates $\mathbf{r} \equiv \mathbf{r}_1 - \mathbf{r}_2$ and $\tau \equiv t_1 - t_2$ in the Keldysh Green's function¹⁸ are Fourier-transformed to obtain momentum and energy variables \mathbf{k} and ϵ , and then perform a gradient expansion with respect to the "center-of-mass" coordinates $\mathbf{R} = (\mathbf{r}_1 + \mathbf{r}_2)/2$ and $t = (t_1 + t_2)/2$. The 2×2 distribution function f_k is obtained¹⁸ by integrating the Keldysh Green's function over energy. For the case of the bilayer graphene Hamiltonian we find that

$$\frac{\partial f_k}{\partial t} + e\mathcal{E} \cdot \frac{\partial f_k}{\partial \mathbf{k}} + i[-\epsilon_k \mathbf{n} \cdot \boldsymbol{\sigma} + \Sigma_k, f_k] = 0, \quad (1)$$

where

$$\Sigma_k = - \sum_{k'} V_{k-k'} f_{k'} \quad (2)$$

is the quasiparticle exchange self-energy. The property that the 2×2 self-energy matrix at one wave vector is simply an interaction-weighted average of distribution function matrices at different wave vectors is a consequence of the model's pseudospin independent interactions.

We consider linear response to an ac electric field, $\mathcal{E} = \mathcal{E}_0 e^{-i\omega t}$, and write $f_k = f_k^{(0)} + f_k^{(1)}$ where $f_k^{(0)} = (1/2) \sum_{\mu=\pm} n_F(\xi_{k\mu})(1 - \mu \boldsymbol{\sigma} \cdot \mathbf{n})$ is the equilibrium distribution function. Here $n_F(x) = \theta(-x)$ is the Fermi function at zero temperature, and $\xi_{k\mu} = \mu \epsilon_k - \epsilon_F$ is the quasiparticle energy rendered from the Fermi level ($\mu=1$ for conduction band and -1 for valence band). Using Eq. (1) we find that

$$-i\omega f_k^{(1)} - i[\epsilon_k \boldsymbol{\sigma} \cdot \mathbf{n} + \Sigma_k, f_k^{(1)}] = S_k + i \sum_{k'} V_{k-k'} [f_{k'}^{(1)}, f_k^{(0)}], \quad (3)$$

where Σ_k now refers to the self-energy evaluated using $f_k = f_k^{(0)}$ in Eq. (2), and

$$S_k = - (e\mathcal{E} \cdot \hat{\mathbf{k}}/2) \sum_{\mu=\pm} [\partial n_F(\xi_{k\mu}) / \partial k] (1 - \mu \boldsymbol{\sigma} \cdot \mathbf{n}) + (1/k) \sum_{\mu=\pm} \mu n_F(\xi_{k\mu}) (e\mathcal{E} \times \hat{\mathbf{k}}) \cdot (\boldsymbol{\sigma} \times \mathbf{n}) \quad (4)$$

is the driving term of the QKE. The first term in Eq. (4) drives intraband transitions and the second term interband transitions. The second term on the right-hand side of Eq. (3) accounts for changes in the self-energy in the nonequilibrium state. Because of this term, Eq. (3) is an integral equation which can only be solved numerically. The distribution function can also be expressed as a sum of intraband and interband contributions,

$$f_k^{(1)} = (\mathcal{E} \cdot \hat{\mathbf{k}}) [A(k) + \boldsymbol{\sigma} \cdot \mathbf{n} B(k) + i(\boldsymbol{\sigma} \times \mathbf{n})_z G(k) + \sigma_z H(k)] + (\mathcal{E} \times \hat{\mathbf{k}})_z [i(\boldsymbol{\sigma} \times \mathbf{n})_z C(k) + \sigma_z D(k) + \boldsymbol{\sigma} \cdot \mathbf{n} E(k) + F(k)], \quad (5)$$

where the $\mathbf{1}$, $\boldsymbol{\sigma} \cdot \mathbf{n}$, $(\boldsymbol{\sigma} \times \mathbf{n})_z$, and σ_z components of each contribution capture, respectively, changes in total density, conduction versus valence-band density difference, interlayer coherence, and layer polarization.

Substituting Eq. (5) into Eq. (3) yields a set of eight coupled equations. We find that E, F, G , and H are all identically zero,

$$A(k) = -B(k) = \frac{ie}{2\omega} \delta(k - k_F), \quad (6)$$

and $C(k)$ and $D(k)$ satisfy the following set of coupled integral equations:

$$\omega C(k) + \delta_k D(k) = \theta(k - k_F) \left[-\frac{e}{k} + \delta \Sigma^z(k) \right], \quad (7)$$

$$\delta_k C(k) + \omega D(k) = \theta(k - k_F) [\delta \Sigma^{\phi,1}(k) + \delta \Sigma^{\phi,2}(k)], \quad (8)$$

where $\delta_k = 2\epsilon_k + \Sigma_{k+} - \Sigma_{k-}$ is the energy needed to create a vertical interband excitation,

$$\Sigma_{k\mu} = - \sum_{\lambda=\pm} \sum_{k'} V_{k-k'} \theta(k_F - \lambda k') (1 + \mu \lambda \cos 2\phi_{k'k}) / 2, \quad (9)$$

is the equilibrium self-energy in band μ , $\phi_{k'k} = \phi_{k'} - \phi_k$, and the nonequilibrium self-energy changes are

$$\delta \Sigma^z(k) = \sum_{k'} V_{k-k'} \cos \phi_{k'k} D(k'), \quad (10)$$

$$\delta \Sigma^{\phi,1}(k) = \sum_{k'} V_{k-k'} \cos \phi_{k'k} \cos 2\phi_{k'k} C(k'), \quad (11)$$

$$\delta \Sigma^{\phi,2}(k) = -i \sum_{k'} V_{k-k'} \sin \phi_{k'k} \sin 2\phi_{k'k} B(k'). \quad (12)$$

Equations (7) and (8) are the equations of motion for the interlayer coherence $C(k)$ and layer polarization $D(k)$ components of the distribution function and describe precession of valence-band pseudospins in the effective magnetic fields due to band-energy separation (δ_k) and to nonequilibrium self-energy corrections. There are three contributions to the nonequilibrium self-energy: $\delta \Sigma^z$, $\delta \Sigma^{\phi,1}$, and $\delta \Sigma^{\phi,2}$. $\delta \Sigma^z$ originates from layer polarization and $\delta \Sigma^{\phi,1}$ from interband coherence. $\delta \Sigma^{\phi,2}$ couples the Drude response [$B(k)$] and the interband response [$C(k)$ and $D(k)$]. This Drude-interband coupling mechanism is one of the principle results of our paper. It appears because the Drude conduction-band Fermi-surface oscillation in an ac electric field changes the e-e interaction exchange potential experienced by precessing valence-band pseudospins outside the Fermi surface.

The current can be evaluated from the perturbed distribution function using $\mathbf{J} = g_v g_s e \text{Tr}[\Sigma_k (1/2) \{ \mathbf{j}_k, f_k^{(1)} \}]$, where $g_v g_s = 4$ is the product of the valley and spin degeneracies and $\mathbf{j}_k = \partial H / \partial \mathbf{k} = -(k/m) [(\boldsymbol{\sigma} \cdot \hat{\mathbf{k}}) \hat{x} - (\boldsymbol{\sigma} \times \hat{\mathbf{k}})_z \hat{y}]$ is the current operator. It then follows from Eq. (5) that the conductivity

$$\sigma(\omega) = -\frac{2e}{\pi m} \int_0^\infty dk k^2 [B(k) + iC(k)]. \quad (13)$$

III. RENORMALIZATION OF DRUDE WEIGHT AND PLASMON FREQUENCY

Before discussing our general results we study the influence of DIC on the Drude weight. At low frequencies the noninteracting response is the out-of-phase oscillations of the Fermi surface with respect to the electric field which is captured by $B(k) \propto i/\omega$. Because of the self-energy correction $\delta \Sigma^{\phi,2}$, there is also an interband response $C(k)$ with the same frequency dependence [See Eq. (8)]. When a momentum relaxation time τ is added to the theory the i/ω contribution to

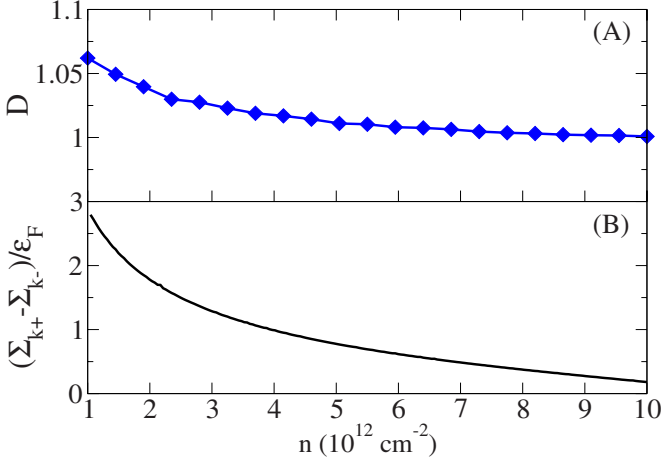


FIG. 1. (Color online) (a) Renormalized Drude weight \tilde{D} versus density n . The enhancement of the Drude weight increases with decreasing density. (b) Band renormalization $(\Sigma_{k+} - \Sigma_{k-})/\epsilon_F$ at $k = k_F$ versus density. These results were evaluated with Coulombic electron-electron interactions and dielectric constant $\kappa=1$, corresponding to a suspended graphene sample.

the conductivity evolves into a Drude peak contribution proportional to $\tau/(1-i\omega\tau)$. The coefficient of this contribution is known as the Drude weight \mathcal{D} . When DIC is included we find that for bilayer graphene the Drude contribution to $\sigma(\omega)$ is

$$\sigma^{\mathcal{D}}(\omega) = \frac{(2e^2\epsilon_F/\pi\hbar)\tilde{D}\tau}{1-i\omega\tau}, \quad (14)$$

where the interaction-induced Drude weight renormalization is given to leading order in e^2 by

$$\tilde{D} = 1 + \frac{e^2}{2\pi\hbar\epsilon_F} \int_{k_F}^{\infty} dk \mathcal{R}\left(\frac{k}{k_F}\right). \quad (15)$$

Here $\mathcal{R}(x) = (4/15x^3)\{(x+1)(x^4-x^2+1)E[4x/(x+1)^2] - (x^2+1)(x-1)^2(x+1)K[4x/(x+1)^2]\}$ and K, E are, respectively, complete elliptic integrals of the first and second kind.

One important consequence of DIC is renormalization of the plasmon frequency. In regular semiconductors with parabolic dispersion, the plasmon frequency ω_p has no long-wavelength interaction renormalization¹⁹ because of Galilean invariance. Since graphene systems are not Galilean invariant, their plasmon frequencies are²⁰ renormalized. Using the well-known relation between the optical conductivity and the polarizability, $\sigma(\omega) = \lim_{q \rightarrow 0} [ie^2\omega\Pi(q, \omega)/q^2]$, the real part of the polarizability for $v_F q \ll \omega$ and $\omega \ll \epsilon_F$ is $\text{Re } \Pi(q, \omega) = (2\epsilon_F\tilde{D}/\pi)(q/\omega)^2$. The renormalized plasmon frequency is then given by the zero of the dielectric function $\epsilon(q, \omega) = 1 - v_q \text{Re } \Pi(q, \omega) = 0$. For BLG we find that

$$\omega_p^2 = 4e^2\epsilon_F\tilde{D}q. \quad (16)$$

Figure 1(a) shows renormalized Drude weights \tilde{D} from the full numerical calculations described below.

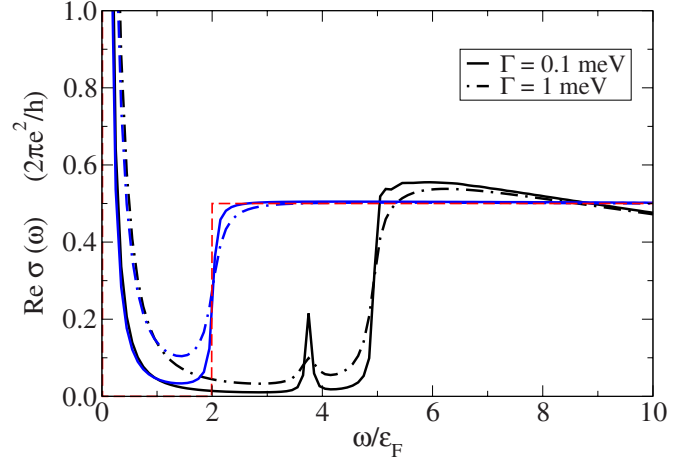


FIG. 2. (Color online) Real part of the optical conductivity $\text{Re } \sigma(\omega)$ vs frequency ω at density $n=10^{12} \text{ cm}^{-2}$ for unscreened (black) and screened (blue/gray) e-e interaction. Results for screening with $\kappa=1$ (corresponding to suspended bilayer graphene) and $\kappa=4$ (corresponding to a bilayer on a SiO_2 substrate) are quantitatively similar and the gray/blue lines show the results for $\kappa=1$. The disorder broadening is taken as $\Gamma \equiv 1/\tau = 0.1 \text{ meV}$ (solid line) and 1 meV (dot-dashed line). The ideal noninteracting case is plotted as the dashed thin gray/red line.

IV. OPTICAL CONDUCTIVITY

The full $\sigma(\omega)$ at arbitrary interaction strength is obtained by solving the coupled integral equations Eqs. (7) and (8) numerically, letting $\omega \rightarrow \omega + i\tau^{-1}$. We can approximately account for screening corrections to our first-order interaction self-energy by replacing the bare Coulomb interaction by its Thomas-Fermi (TF) statically screened counterpart.

When screening is neglected, interactions significantly alter $\sigma(\omega)$ in three respects, as illustrated in Fig. 2. First, the interband absorption threshold is changed dramatically from $\omega = 2\epsilon_F$ to $\omega \approx 5\epsilon_F$. This effect is analogous to band-gap renormalization in regular semiconductors, with the Fermi level playing the role of a gap because of Pauli blocking. The threshold shift is equal to $\Sigma_{k_F+} - \Sigma_{k_F-}$ [Fig. 1(b)]. Second, the value of $\sigma(\omega)$ is no longer universal above the absorption threshold; instead it shows a decreasing trend with ω , first reaching above and then dropping below the noninteracting value $e^2/2\hbar$. Third, an absorption peak appears below the threshold. This *Mahan exciton*²¹ feature is a well-understood artifact of our simple self-energy approximation. Because of electron-scattering processes (including Fermi-surface fluctuations due to intraband electron-hole excitations²² and impurity scattering) in the conduction band not captured by our self-energy approximation, the Mahan exciton is invariably unstable. In Fig. 2 we illustrate broadening of the Mahan exciton due to disorder.

The results obtained when we screen the interactions in our self-energy expression using a TF approximation are shown in gray in Fig. 2. The TF screening wave vector for BLG is given by $q_{\text{TF}} = 4me^2/\kappa$, a constant independent of electron density. Surprisingly, we find that with screening (1) the interband absorption threshold shift nearly disappears, (2) $\text{Re } \sigma(\omega) \approx e^2/2\hbar$ above the threshold, and (3) the Mahan

exciton bound state vanishes. In short, the optical conductivity $\text{Re } \sigma(\omega)$ behaves essentially like that of a noninteracting system.

To shed light on this result, we observe that the TF wave vector $q_{\text{TF}} \approx 2.62 \times 10^9 \text{ m}^{-1}/\kappa$ for BLG is extremely large compared to all momentum scales of electronic transitions and is, in fact, greater than the momentum cutoff $k_c = \sqrt{2m\gamma_1}$ for both suspended ($\kappa=1$) and substrate-mounted ($\kappa=4$) bilayers. In a TF screening approximation: $V_q \approx 2\pi e^2/q_{\text{TF}}$ behaves as short-range interaction V_0 in the regime of interest $\varepsilon_F, \omega < \gamma_1$, with the consequence that in Eqs. (9)–(12) the band renormalization

$$\Sigma_{k_+} - \Sigma_{k_-} \propto V_0 \int d\phi_{k'k} \cos 2\phi_{k'k}, \quad (17)$$

and the nonequilibrium self-energies

$$\begin{aligned} \delta\Sigma^z &\propto V_0 \int d\phi_{k'k} \cos \phi_{k'k}, \\ \delta\Sigma^{\phi,1} &\propto V_0 \int d\phi_{k'k} \cos \phi_{k'k} \cos 2\phi_{k'k}, \\ \delta\Sigma^{\phi,2} &\propto V_0 \int d\phi_{k'k} \sin \phi_{k'k} \sin 2\phi_{k'k} \end{aligned} \quad (18)$$

all vanish. Therefore, strong screening in BLG restores the optical conductivity essentially to its noninteracting value. This remarkable result is peculiar to BLG, since its double-chirality gives rise to spinors with s -wave and d -wave components (rather than s wave and p wave as in SLG), which do not couple to p -wave optical dipole transitions through an s -wave short-range interaction. For the case of gapped BLG, since our theoretical results follow principally from pseudospin chirality and will not be influenced by an external

potential—we expect that on the basis of current results, interaction effects in these gapped systems with finite doping will also be suppressed.

Finally we comment on the experimental implications of our findings. We interpret the weak experimental^{10–13} absorption threshold features as evidence for short-range screened e-e interactions. We recognize, however, that the static screening we use could overstate the reduction in interaction range and that interaction effects are likely to persist to some degree in $\sigma(\omega)$, especially in suspended bilayers for which the dielectric-environment portion of the screening is absent. Interaction effect could be identified experimentally via the ω_p renormalizations we predict, for example using electron energy-loss spectroscopy studies of suspended samples. We also remark that in employing the massive two-band model for BLG, we have neglected transitions to the two bands which are respectively located at an energy $\approx \gamma_1$ above (below) the conduction (valence) band described in the two-band model, and interaction effects might be more pronounced in such intra-conduction band and intra-valence band transitions.

V. CONCLUSION

In conclusion, we have developed a theory for the e-e interaction effects on the optical conductivity $\sigma(\omega)$ of doped bilayer graphene. We discover a coupling effect which couples the Drude and interband response of the optical conductivity, and an accompanying renormalization of the leading-order plasmon frequency. We also find that screening dramatically suppresses band renormalization and excitonic effects, restoring $\sigma(\omega)$ very close to the universal value $e^2/2\hbar$ above the absorption threshold.

ACKNOWLEDGMENTS

W.-K. thanks Qian Niu for useful discussions. This work was supported by the Welch Foundation and by the DOE.

- ¹A. K. Geim and K. S. Novoselov, *Nature Mater.* **6**, 183 (2007).
- ²E. McCann and V. I. Fal'ko, *Phys. Rev. Lett.* **96**, 086805 (2006).
- ³J. Nilsson, A. H. Castro Neto, F. Guinea, and N. M. R. Peres, *Phys. Rev. Lett.* **97**, 266801 (2006).
- ⁴D. S. L. Abergel and V. I. Fal'ko, *Phys. Rev. B* **75**, 155430 (2007).
- ⁵E. J. Nicol and J. P. Carbotte, *Phys. Rev. B* **77**, 155409 (2008); L. Benfatto, S. G. Sharapov, and J. P. Carbotte, *ibid.* **77**, 125422 (2008).
- ⁶T. Stauber, N. M. R. Peres, and A. H. Castro Neto, *Phys. Rev. B* **78**, 085418 (2008).
- ⁷L. M. Zhang, Z. Q. Li, D. N. Basov, M. M. Fogler, Z. Hao, and M. C. Martin, *Phys. Rev. B* **78**, 235408 (2008).
- ⁸H. Haug and S. W. Koch, *Quantum Theory of the Optical and Electronic Properties of Semiconductors* (World Scientific, Singapore, 2004).
- ⁹R. Zimmerman, *Many-Particle Theory of Highly Excited Semiconductors* (Teubner, Leipzig, 1987).
- ¹⁰F. Wang, Y. Zhang, C. Tian, C. Girit, A. Zettl, M. Crommie, and Y. R. Shen, *Science* **320**, 206 (2008).

- ¹¹Z. Q. Li, E. A. Henriksen, Z. Jiang, Z. Hao, M. C. Martin, P. Kim, H. L. Stormer, and D. N. Basov, *Phys. Rev. Lett.* **102**, 037403 (2009).
- ¹²A. B. Kuzmenko, E. van Heumen, D. van der Marel, P. Lerch, P. Blake, K. S. Novoselov, and A. K. Geim, *Phys. Rev. B* **79**, 115441 (2009).
- ¹³Y. Zhang, T.-T. Tang, C. Girit, Z. Hao, M. C. Martin, A. Zettl, M. F. Crommie, Y. R. Shen, and F. Wang, *Nature (London)* **459**, 820 (2009).
- ¹⁴Giovanni Borghi, Marco Polini, Reza Asgari, and A. H. MacDonald, *Solid State Commun.* **149**, 1117 (2009).
- ¹⁵A. B. Kuzmenko, I. Crassee, D. van der Marel, P. Blake, and K. S. Novoselov, *Phys. Rev. B* **80**, 165406 (2009).
- ¹⁶A gap can be induced in bilayer graphene by an external electric field which produces an electric potential difference between the two layers and breaks inversion symmetry. See for example Refs. 13 and 15, and work cited therein. In this article we focus on the balanced bilayer case in which inversion symmetry is maintained.

¹⁷We are neglecting the small difference in interaction energy between electrons in the same layer and electrons in different layers.

¹⁸J. Rammer and H. Smith, *Rev. Mod. Phys.* **58**, 323 (1986).

¹⁹W. Kohn, *Phys. Rev.* **123**, 1242 (1961).

²⁰M. Polini, A. MacDonald, and G. Vignale, arXiv:0901.4528 (unpublished).

²¹G. D. Mahan, *Phys. Rev.* **153**, 882 (1967); **163**, 612 (1967).

²²J. Gavoret P. Nozières, B. Roulet, and M. Combescot, *J. Phys. (France)* **30**, 987 (1969).